DEUTSCHES ELEKTRONEN-SYNCHROTRON

DESY

DESY 65/7

August 1965
Experimente

ELECTROPRODUCTION OF π-MESONS AND PHOTOPRODUCTION OF DIPIONS

by

H. Blechschmidt, B. Elsner, K. Heinloth,
A. Ladage, J. Rathje, D. Schmidt

(Vorh. in: Hamburg 1965. International Conference on Electron and Photon Interactions. Vol. 2. S. 173-177.)

2 HAMBURG-GR. FLOTTBEK 1, NOTKESTIEG 1

Introduction:

In a spark chamber experiment at DESY we have measured the electroproduction of π-mesons (1, 2, 3) with primary electrons of 5.2 GeV/c momentum, looking for coincidences between the scattered electron and at least one π-meson.

At the same time photoproduction of dipions was observed using bremsquanta produced by the electrons in the hydrogen target.

In part 1 the experimental set-up and the parameters of the experiment are described.

In part 2 we discuss briefly the main physical problems of electroproduction and give results of our first measurement of electroproduction of single and multiple π-mesons.

In part 3 we report the result of photoproduction of dipions in the same run.

I Experimental set-up:

a. The electron beam:

A schematic of the layout of the experiment is shown in fig. 1.

In an internal target T_1 of 0.1 rad. length a beam of bremsstrahlung is produced, which is converted by a second target T_2 of variable thickness into an electron-positron beam. After focusing the e-beam by a quadrupol doublet Q_1 Q_2 a small momentum band is cut out by a collimator C_1 behind a momentum defining bending magnet M_1. A second bending magnet M_2 compensates the momentum dispersion caused by M_1, and 3 more quadrupols focus the beam into the region of the experimental target T_3.

We used an electron beam of 5.2 GeV/c momentum, with an momentum spread of $\pm$ 50 MeV/c.

The size of the beam in the region of the experimental target was about 10 x 10 mm. The beam divergence was about $\pm$ 1 mrad.

A collimator C_2 40 mm wide near the experimental target was used to get rid of high momentum tails on both sides of the beam.

The beam contamination by this collimator was checked and found to be negligible.

The intensity used during the experiment was about $2 \cdot 10^3$ electrons/pulse, with an effective pulse length of about 300 μsec.

The intensity was monitored by an ionisation-chamber in front of C_2. The absolute accuracy was given by a rough comparison with a calibrated ionisation chamber to $\pm$ 10%.

b. The spark chamber set-up.

A detailed view of the spark chamber arrangement is shown in fig. 2. The arrangement is similar to the ones built at CERN (4) and at CEA (5).

The electron beam hits a liquid hydrogen target of 0.02 radiation length. The angle of production of both detected particles was measured in 2 thin-plate spark chambers behind the target. The momentum of the particles was analyzed by measuring the deflection of the particles in a homogenous magnetic field of 16 kGauss in 2 more thinplate spark chambers behind the magnet. The solid angle of the detection system of $\pm$ 17 degrees horizontally and $\pm$ 2.2 degrees vertically was determined by the magnet aperture of 150 cm x 30 cm.

The primary electron beam was buried in a heavy metal beam catcher inside the magnet after having passed through holes in the first 2 spark chambers. The smallest angle under which particles could be detected was determined by the beam catcher to about 2^{o} .

In a 5^{th} thick-plate spark chamber electrons are discriminated against heavier particles by showering up. The efficiency of this chamber was tested with an e-beam to be better than 90%.

For triggering the spark chambers a 5-fold coincidence was required between scintillation counters 1 + 2 indicating 2 particles in front of the magnet, and 3 + 4 indicating 2 particles behind the magnet, and 5 indicating at least one particle in the shower chamber. The coincidence was vetoed by 2 anticounters 6 + 7 excluding background events from outisde the target.

The efficiency of the trigger counters was roughly checked to be near to 100%.

The track efficiency of the spark chambers was 100% requiring not all gaps to fire.

One more source of error had to be investigated: electrons make bremsstrahlung in the material of our set-up.

The fraction of electrons which loose more than 50 MeV energy by making bremsstrahlung in front of the momentum analyzing magnet was calculated to be 18%. This value was proofed experimentally.

Because we had no Cerenkov-counter available we could not discriminate π-mesons from heavier particles. From recent measurements (15) we estimate K-contamination to be about 5%. The contamination by protons of high momenta should be negligible.

Only particles with momenta $p \geq 700$ MeV were accepted.

The contamination of μ -mesons mainly arising from decay of π-mesons was about 4%.

Two views of each of all 5 spark chambers are photographed onto a 35 mm reversal-film.

Fig. 3 shows a typical event of e-π-production. On the picture the relative distances between spark chamber 1 and 2 respectively 3 and 4 are preserved for easier scanning.

The events were measured on two digitised measuring tables coupled to an IBM card-puncher. (6).

The calculation was done on the IBM-7044 computer at DESY.

Programs were written (7) for momentum analysis of the particles going through the field of the used magnet and for the kinematics of the reactions investigated.

II Physical Problems and Results.

a. Discussion of the physical problem.

Till now we have measured 70 e,π^{+}_{-} events. The results are given here.

The events arise from single and multiple π-production according to

$$e^- + p^+ \rightarrow e^- + N + n \cdot \pi \qquad n \geq 1.$$

We are detecting the momenta of the scattered electron and of 1 charged π-meson. Therefore single π-production can be analyzed completely, because we have all kinematical information.

In the following we assume that the electron interacts via single-photon exchange. In the range of the mass-square of the virtual photon up to about 0.5 GeV^2 which covers nearly all our data this assumption should be valid.(8).

The reactions may be shown in the following graph.

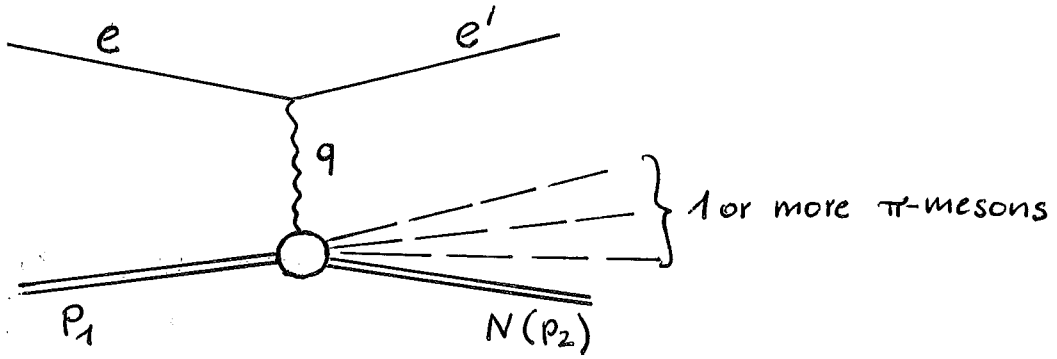

e, e' = four-momenta of primary and scattered electron

q = four-momentum of the virtual photon

$\lambda = (e - e')^2$

$k_o \approx e_o - e'_o$

$\vartheta = \sphericalangle (e, e')_{L.S.}$

Therefore electroproduction can be separated into the emission of a virtual photon and photoproduction with this virtual photon (9).

Virtual photons arising from the scattering of electrons are polarized. The polarization has a transversal and a longitudinal component. The transversal component is linearly polarized in the production plane. The degree of linear polarization (1)

$$(1) \qquad \varepsilon = \frac{\lambda/k_o^2 \cdot \cot^2 \frac{\vartheta}{2}}{2 + \lambda/k_o^2 \cot^2 \frac{\vartheta}{2}}$$

is shown in fig. 4 as a function of the four momentum square λ, the energy transfer k_o and the scattering angle ϑ of the electron.

The average polarization in the range of $1 \leq k_o \leq 4$ GeV, as accepted in our experiment is about 0.8.

In the region of $\lambda \leq 0.5$ GeV^2 given in the experiment the ratio of longitudinal and transversal component is of the order of a few percent.

The cross-section for photoproduction with virtual photons can be written as a sum of the parts (1, 10, 11, 12) arising from the different polarization states.

$$(2) \qquad \sigma = \sigma_u + \sigma_P + \sigma_L + \sigma_I$$

where σ_u is the photoproduction cross-section with transversely unpolarized virtual photons,

σ_P is the photoproduction cross-section with transversely polarized virtual photons,

σ_L is the photoproduction cross-section with longitudinally polarized photons,

and σ_I is the interference term between σ_L and $\sigma_u + \sigma_I$.

Because of the small virtual mass of the photon the contribution of the longitudinal component to the cross-section is small, and we can compare the photoproduction cross-sections with virtual and real photons. Besides

kinematical factors the σ_i contain dynamical form factors (10).

Because the form factors apply differently to various models of photoproduction, one is able to investigate these models. The determination of the different form factors is possible by the measurement of coincidences between scattered electron and produced π-mesons.

This method can be applied not only to the electroproduction of single π-mesons but also to the electroproduction of π-meson- and nucleon resonances.

b. Experimental results:

In fig. 5a, b plots are given of the missing mass M_m for π^+ and π^--production according to

$$e^- + p \rightarrow e^- + \pi^+ + N'(M_m)$$

The resolution of the missing mass is given by the experimental inaccuracies to about $\pm$ 60 MeV.

In the case of π^+ production (fig. 5a) the bare nucleon mass is clearly separated from higher masses, thus indicating production of a single π^+ meson.

In the following we treat events with a missing mass $900 \leq M_m \leq 1100$ MeV as single π-production.

The energy spectra of the virtual photons for single π- and multiple π-production are shown in fig. 6a resp. 6 b.

The shape of the energy-spectrum is strongly influenced by the acceptance of our detection system. For multiple π-production the acceptance depends strongly on the production mechanism. The acceptance for multiple π-production is not taken into account, because we cannot make a clear decision about the production mechanism.

The mass-square of the virtual photons for single π-production is plotted in fig. 7a, for multiple π-production in fig. 7b and c respectively. The lower limit of λ was given by the momentum and angle acceptance to $\lambda \gtrsim 0.02\ \mathrm{GeV}^2$.

The solid curve in fig. 7a is calculated by comparing electroproduction with photoproduction with unpolarized photons (10) in the limit of small momentum square of the photon

$$\frac{|\lambda|}{k_o^2} \ll 1$$

where the virtual photon is treated as a real one.

In this limit the electroproduction cross-section is equal to the photoproduction cross-section multiplied with a function H, which contains kinematical factors.

$$(3)\quad \left(\frac{d\sigma}{d\lambda\, ds_o\, dt_o}\right)_{e+p\to e+n+\pi^+} = H(s_o, s, \lambda) \cdot \left(\frac{d\sigma(s_o, t_o)}{dt_o}\right)_{\gamma+p\to n+\pi^+}$$

where $S_o = (p_1 + q)^2$
$t_o = (p_1 - p_2)^2$
$S = (p_1 + e)^2$

Because of our small number of events of single π^+-production, we first integrated over S_o and t_o in the range given in our experiment and did the comparison in the following form

$$(4)\quad \left(\frac{d\sigma}{d\lambda}\right)_{e+p\to e+\pi^+ n} = H'(s, \lambda) \cdot \sigma_{\gamma+p\to\pi^+ n}$$

The experimental values for single π^+ photoproduction were taken from (13) and extrapolated up to a photon energy of 2.5 GeV.

If one assumes a variation of the form factor for e-π-production (11) like $G_M^2(\lambda)$ for elastic e-scattering (8), then the electroproduction cross-section in eq. 4 is reduced by the factor $G_M^2(\lambda)$. This is indicated in fig. 7a by the dashed curve.

Our data seem to fit the general shape of the calculated curve. With our poor statistics we cannot yet draw a conclusion about the influence of the form factor.

Investigation of the production mechanism:

Assuming one π-exchange for the photoproduction of single π-mesons with virtual photons the π-mesons should show a dependence of the production angle, referred to the direction of the virtual photon $\vartheta_{\pi\lambda}$

like $$\frac{\sin^2 \vartheta_{\pi\lambda}}{(1-\beta_\pi \cos \vartheta_{\pi\lambda})^2} \qquad (14)$$

To compare the production angle of each of our events with the one π-exchange model we calculated the mean angle $\overline{\vartheta}_{\pi\lambda}$ according to the distribution given above in the momentum range of the produced π-mesons.

Fig. 8 shows the distribution of $\vartheta_{\pi\lambda}$ against $\frac{p_\pi}{\overline{\vartheta}_{\pi\lambda}}$. The dashed curve represents the dependence of the mean angle $\overline{\vartheta}_{\pi\lambda}$.

We conclude that our data are not in disagreement with one-π-exchange.

To see whether the single π-meson might be produced by excitation of a nucleon resonance N^* and subsequent decay of the resonance we plotted the mass $M^*_{\pi N}$ of the resonance in fig. 9. $\left(M^{*2} \approx M_p^2 + 2M_p (e_o - e_o')\right)$.
It has to be mentioned that the lowest mass M^* which we can detect in our

experimental set-up is about 1600 MeV.

Again poor statistics do not let us draw a conclusion.

For multiple π-production under assumption of excitation of a nucleon-resonance M^* fig 10 shows a distribution of the mass M^* of this resonance.

To see whether a possible nucleon resonance N^* might first decay into a π-meson and a subsequent other resonant nucleon state N^1 fig. 11 shows a plot of M^* versa M^1.

Fig. 9-11 show no clear evidence for excitation of a nucleon resonance N^* and subsequent decay into another resonant nucleon state, or for production of a single peripheral π-meson with excitation of a nucleon resonance.

III Photoproduction of Dipions.

To check the measured cross-sections we have also analyzed the dipion events produced at the same time by real γ's from bremsstrahlung of the electrons in the hydrogen target.

In the following part, the results of our dipion measurements are given:

Fig.5 shows the mass-plot of all measured dipion events. Because the Cerenkov-counter was not yet ready for our last run the result is contaminated by K-meson pairs of approximately 5%. The dotted curve indicates the geometrical acceptance of the detection system.

The ρ-meson peak shows clearly up around a dipion mass of 720 MeV with a width of about $\pm$ 50 MeV.

From the massplot we estimate the background to about30%. Subtracting this background we calculated a total cross-section for photoproduction of ρ^o-mesons in the region of $3 \leq E_\gamma \leq 5.2$ GeV.

$$\sigma_{tot} = 12/\text{ubarn}$$

In this preliminary analysis we estimate an accuracy of $\pm$ 50% because of the error of the calibration of the primary beam and because of our rough calculation of the acceptances. The total cross-section seems to be constant in the given region of the γ-energy within $\pm$ 30%.

We also measured dipion production on a carbon target. The total cross-section per nucleon is the same as using a hydrogen target.

The accuracy of the ratio of both cross-sections $\sigma_{C\text{-Nucleon}}/\sigma_H$ is given by pure statistics to $\pm$ 15%.

The results are in good agreement with recent measurements of the CEA bubble chamber group (15) and the DESY bubble chamber cooperation (16).

Conclusion:

Although the data from our first run are poor, we can already draw a few conclusions.

A comparison of electroproduction and photoproduction of single π-mesons shows, that at least in the limit of small four-momentum square of the virtual photon electroproduction can be treated as production of virtual photons and subsequent photoproduction.

The mechanism of electroproduction of single π-mesons seems to be in reasonable agreement with the one-π-exchange model.

In single and multiple π-production with energies of the virtual photon above 1 GeV the excitation of nucleon resonances does not seem to give the main contribution to the cross-section.

We go on to investigate electroproduction of mesons. We have a good chance to get much more information by improving our experimental set-up.

Acknowledgements:

We wish to thank the machine group and all technical groups of DESY for their continuous help.

We also thank our students, scanners and technicians for their tedious work.

Spark-chamber setup

fig. 2

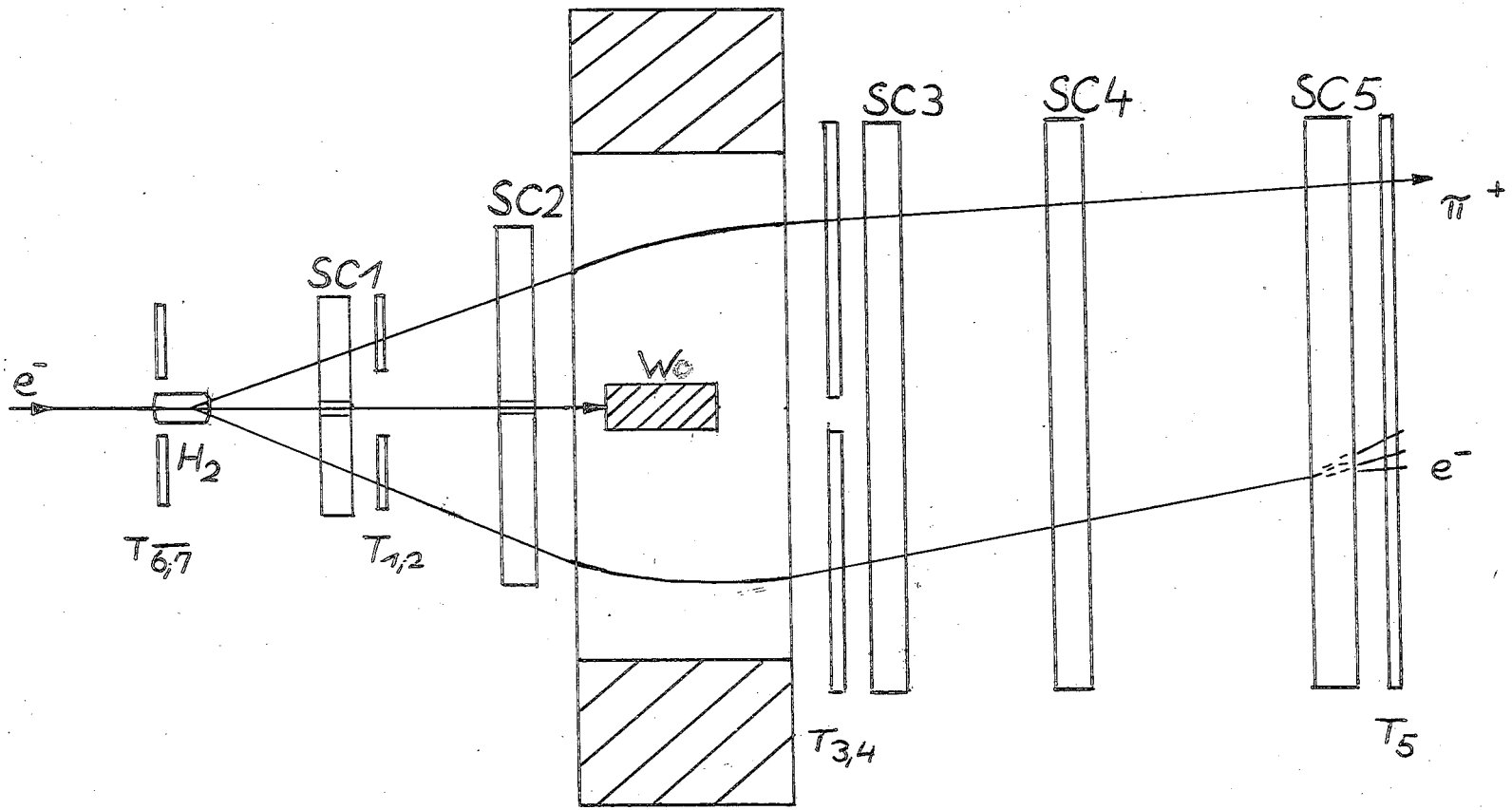

HAMMURABI

General Lay-out

fig. 1

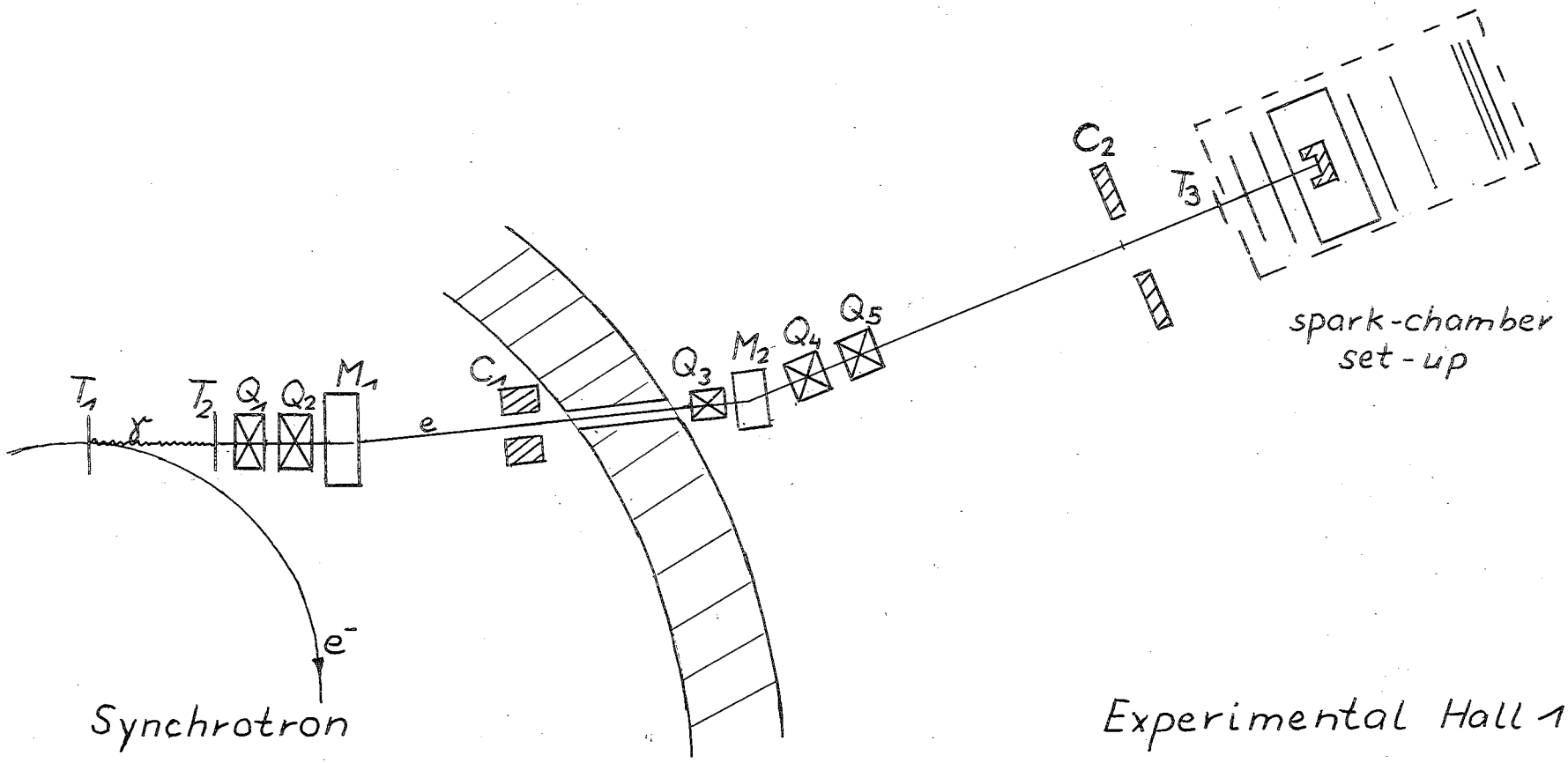

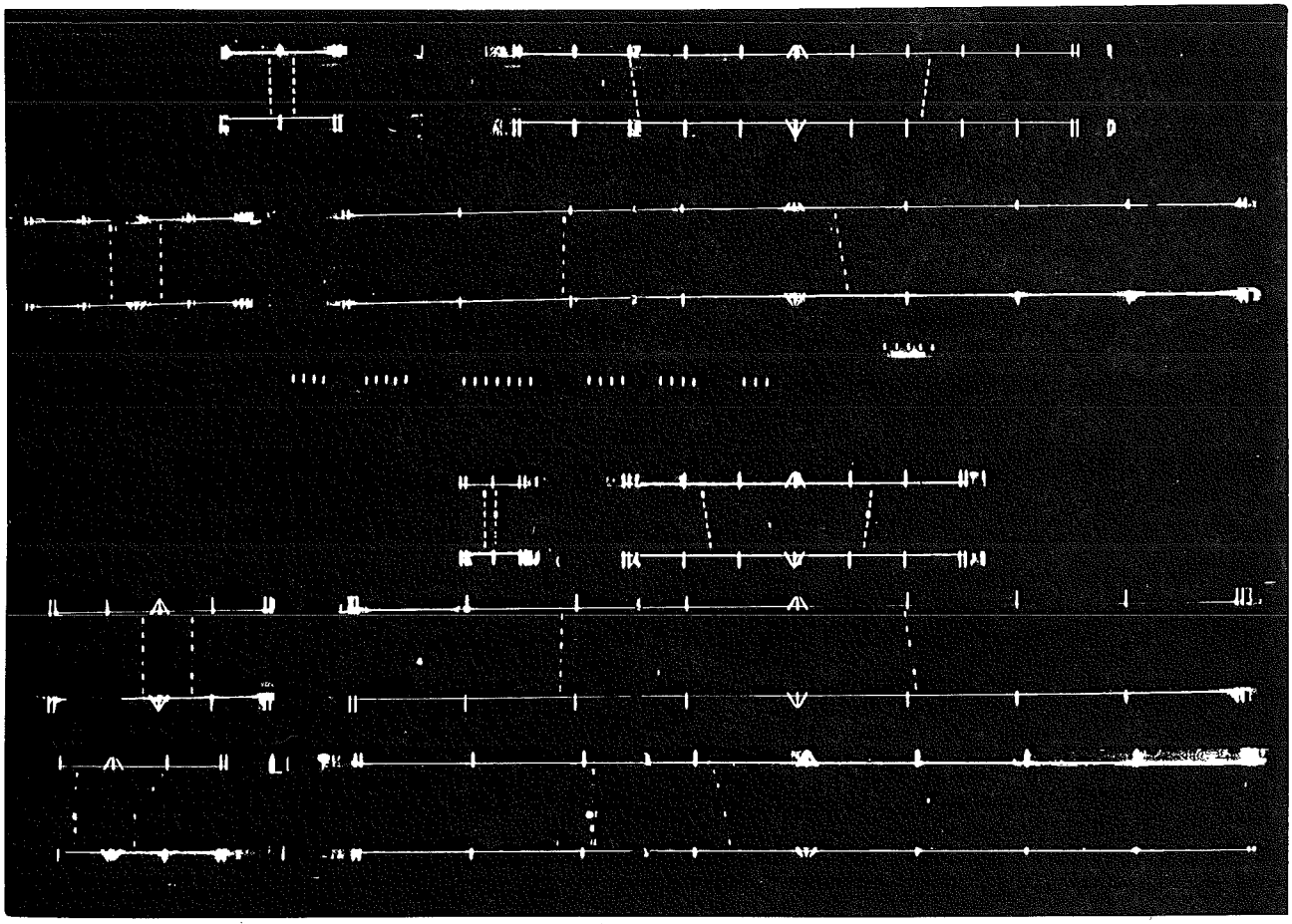

fig. 3

Linear Polarisation of the Transversal Component of the Virtual Photons.

fig. 4

$e_0 = 5.0$ GeV

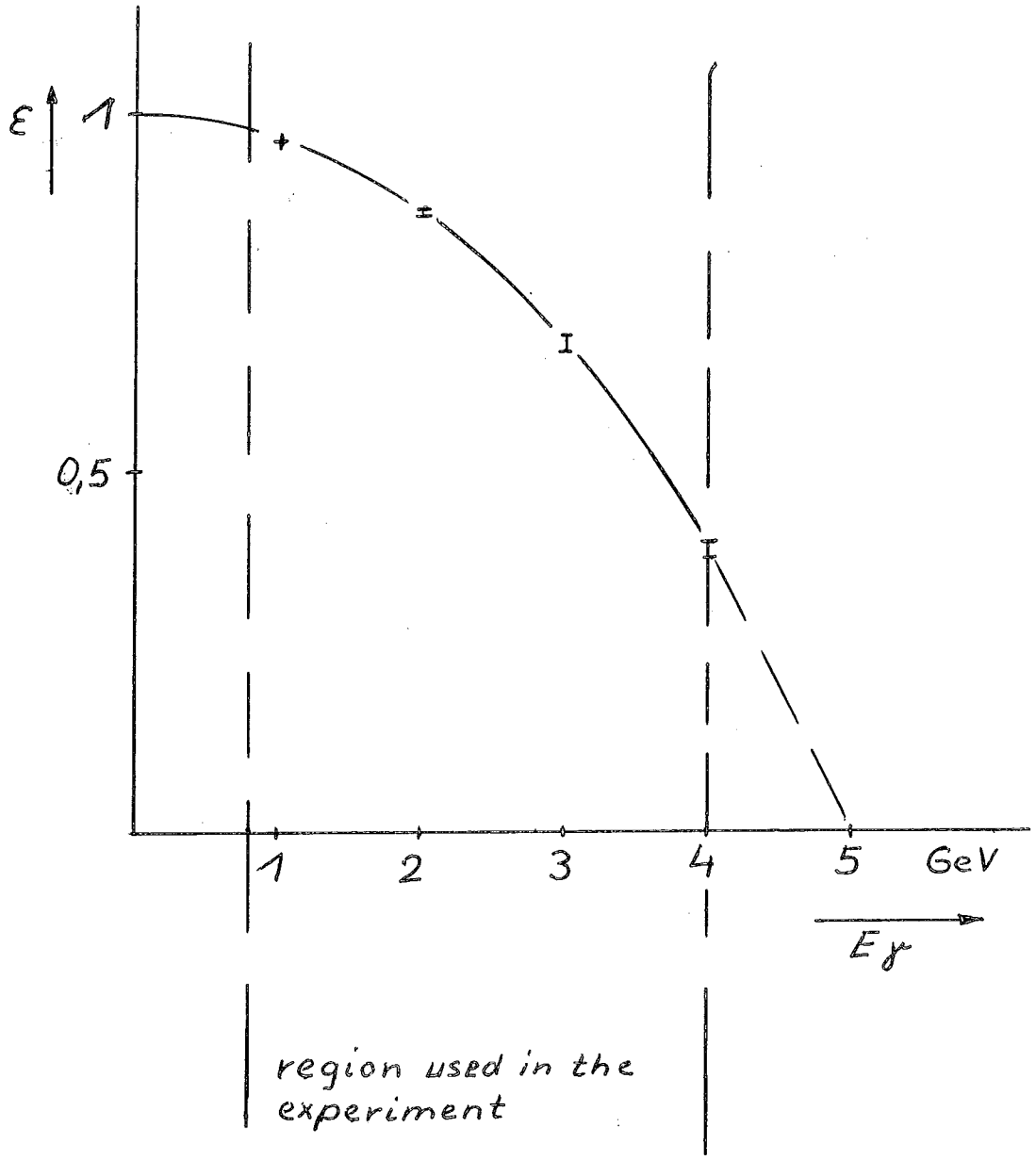

I) $0.02 \leq \lambda \leq 0,5$ GeV^2

Missing Mass Plot

fig. 5

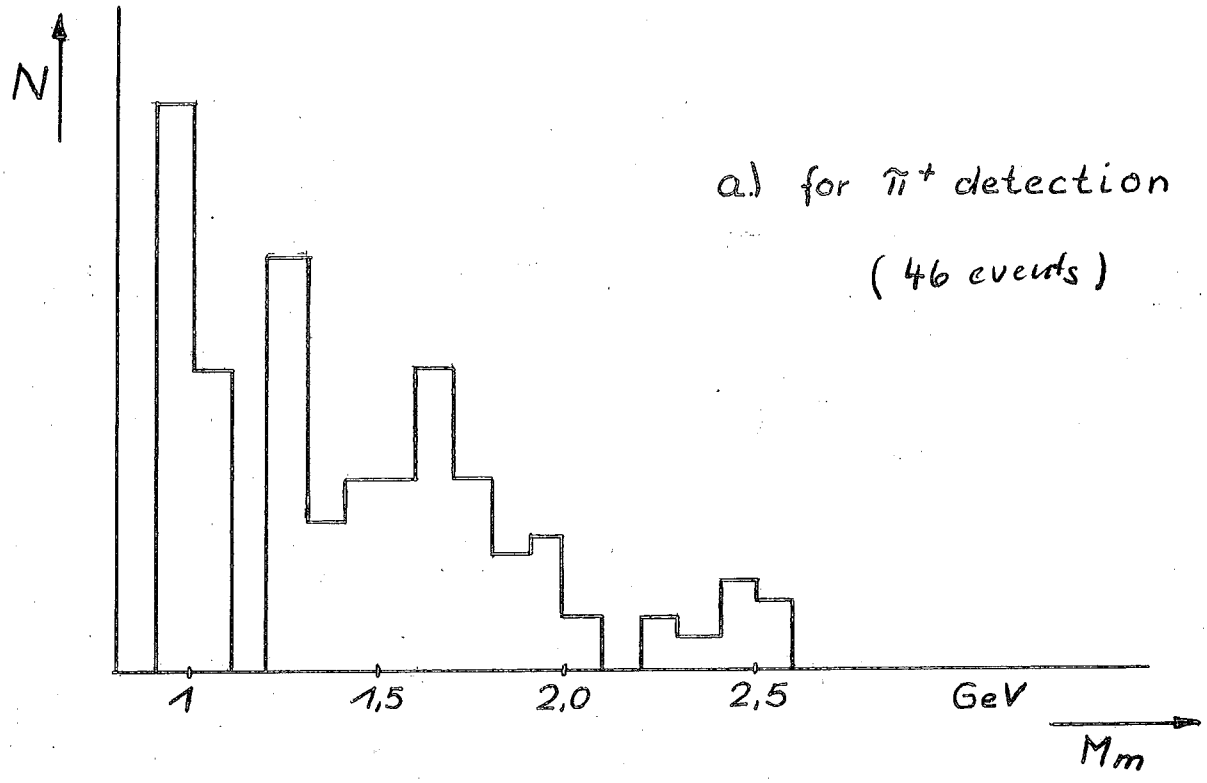

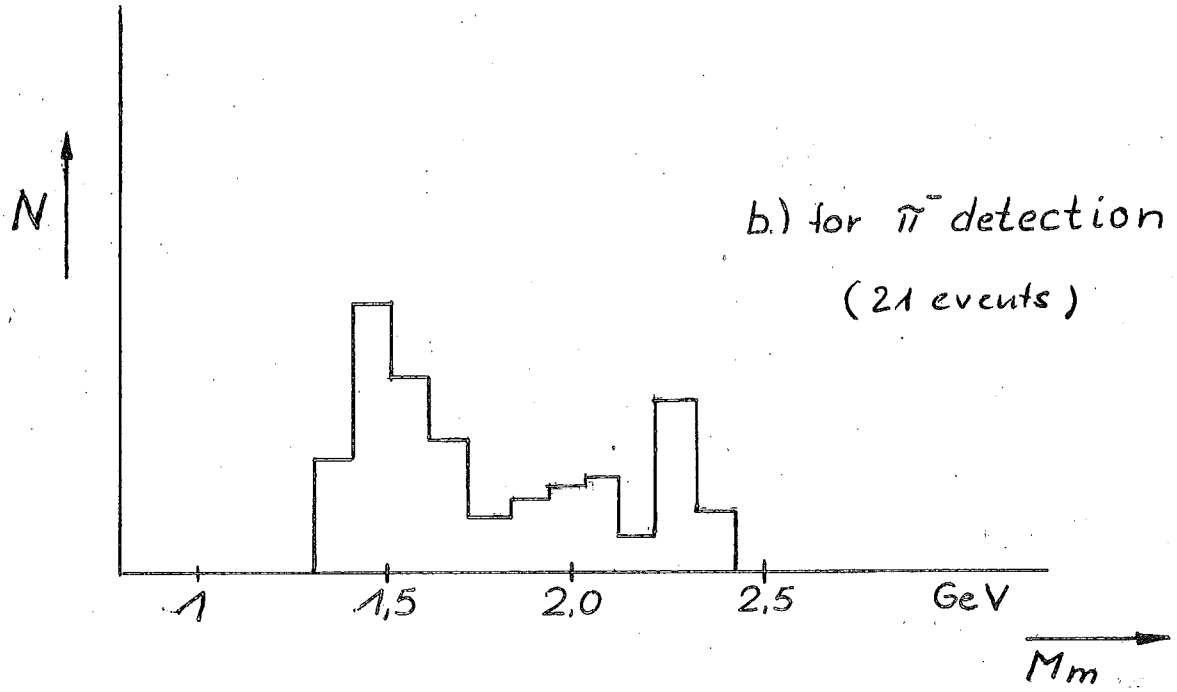

Energy-spectra of virtual photons

fig. 6

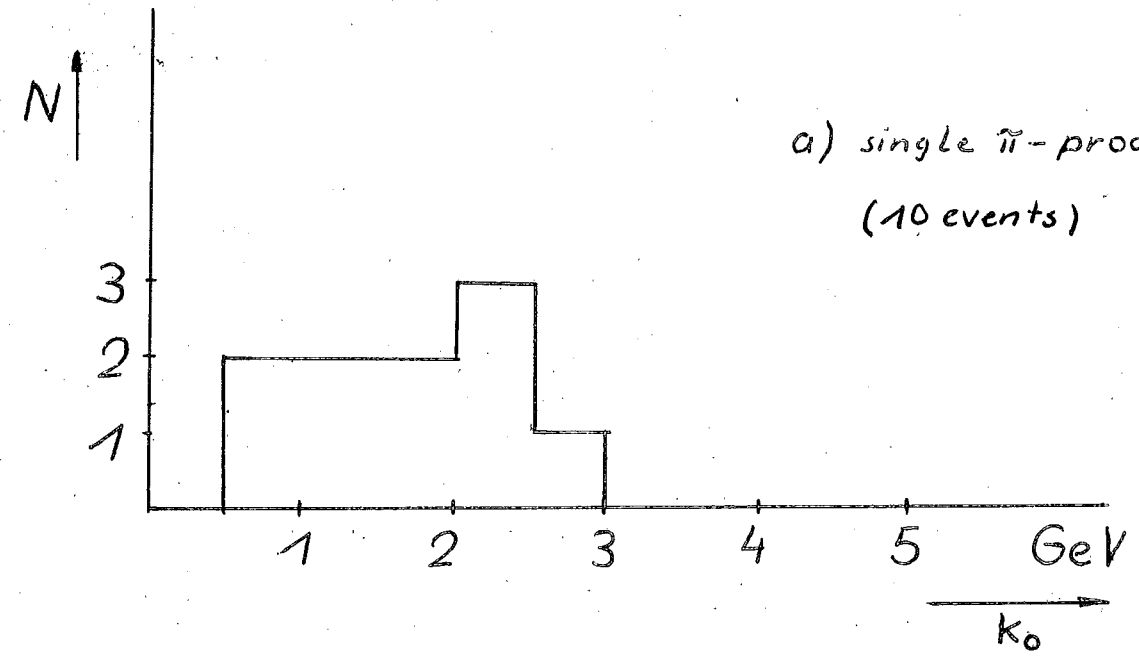

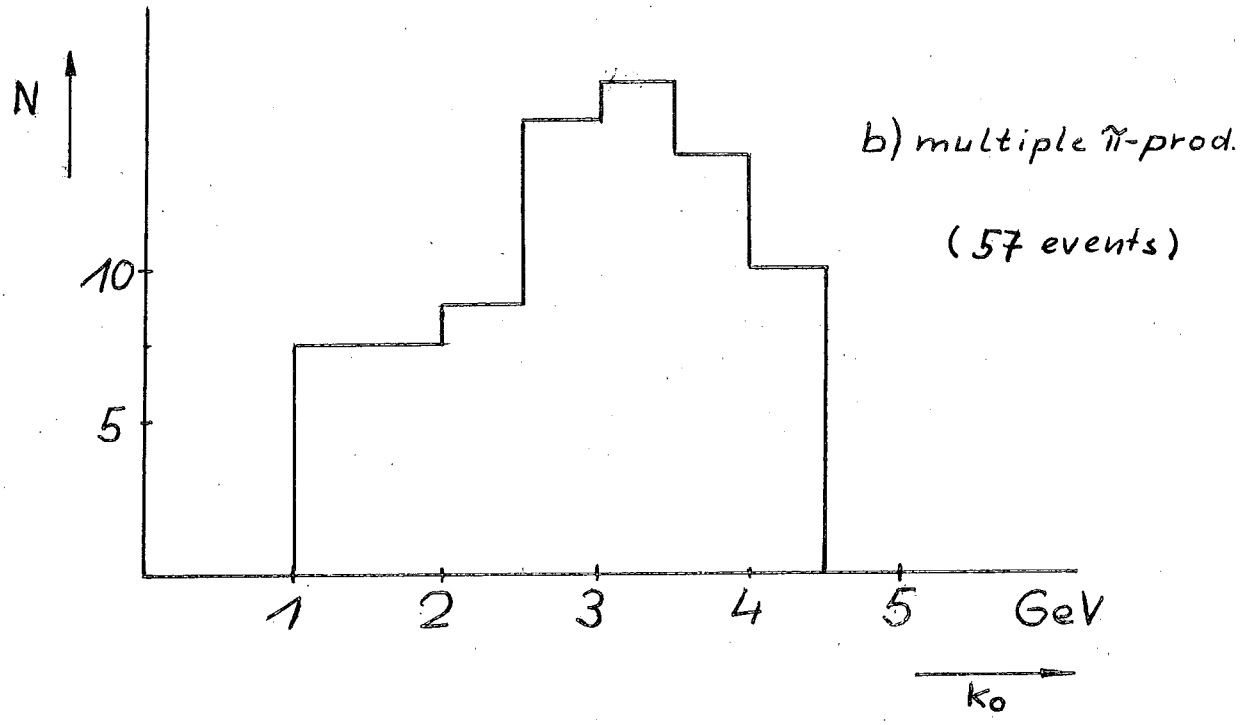

Electroproduction Cross-Section of Single π^+-Mesons as a Function of the Four-Momentum-Square of the Virtual Photon

fig. 7a

(10 events)

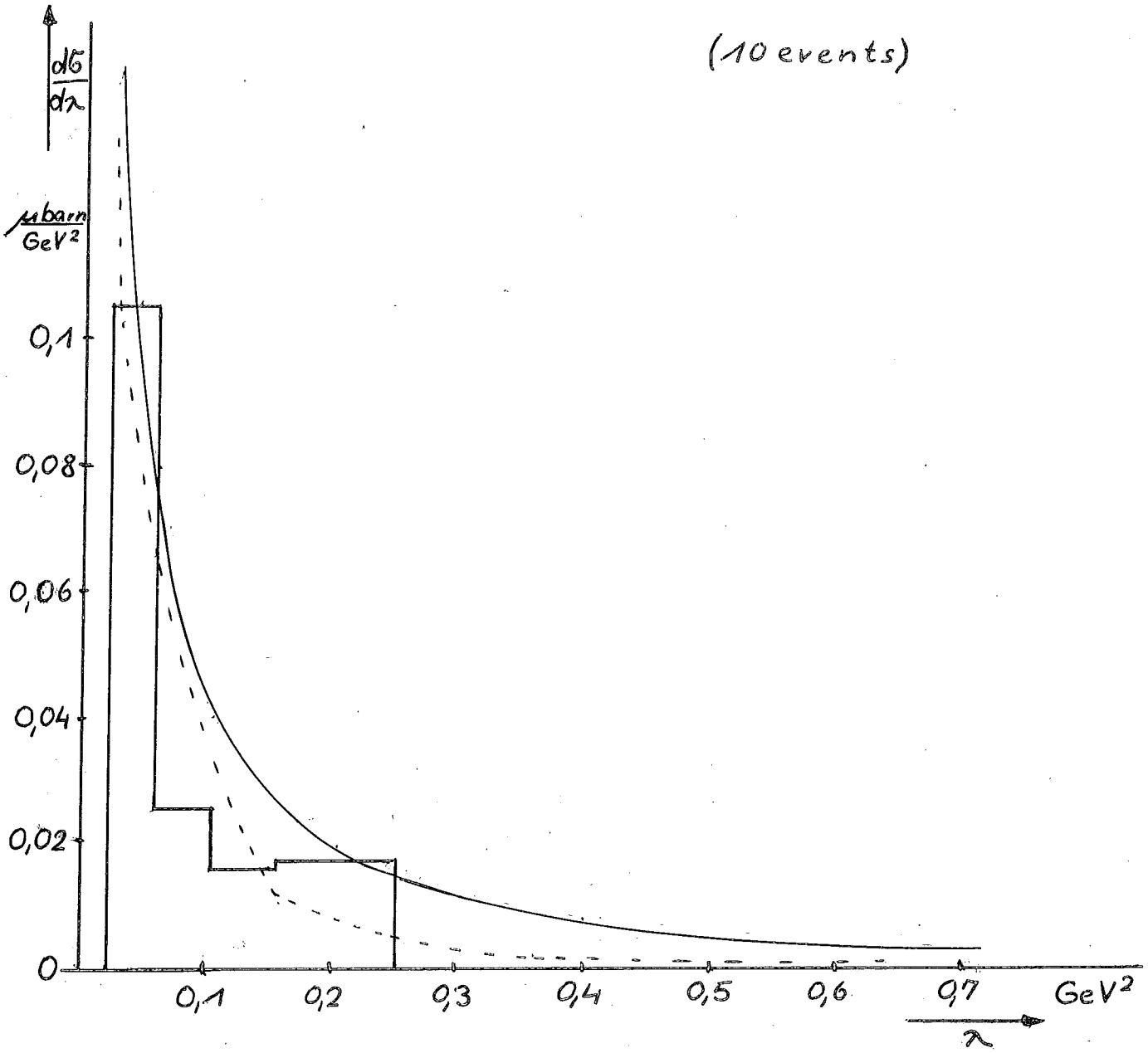

λ [GeV²]	G_M/μ_p
0,05	0,9
0,15	0,65
0,35	0,45
0,65	0,27

Plot of the Four-Momentum square λ of the Virtual Photons in Multiple $\tilde{\pi}$-Production

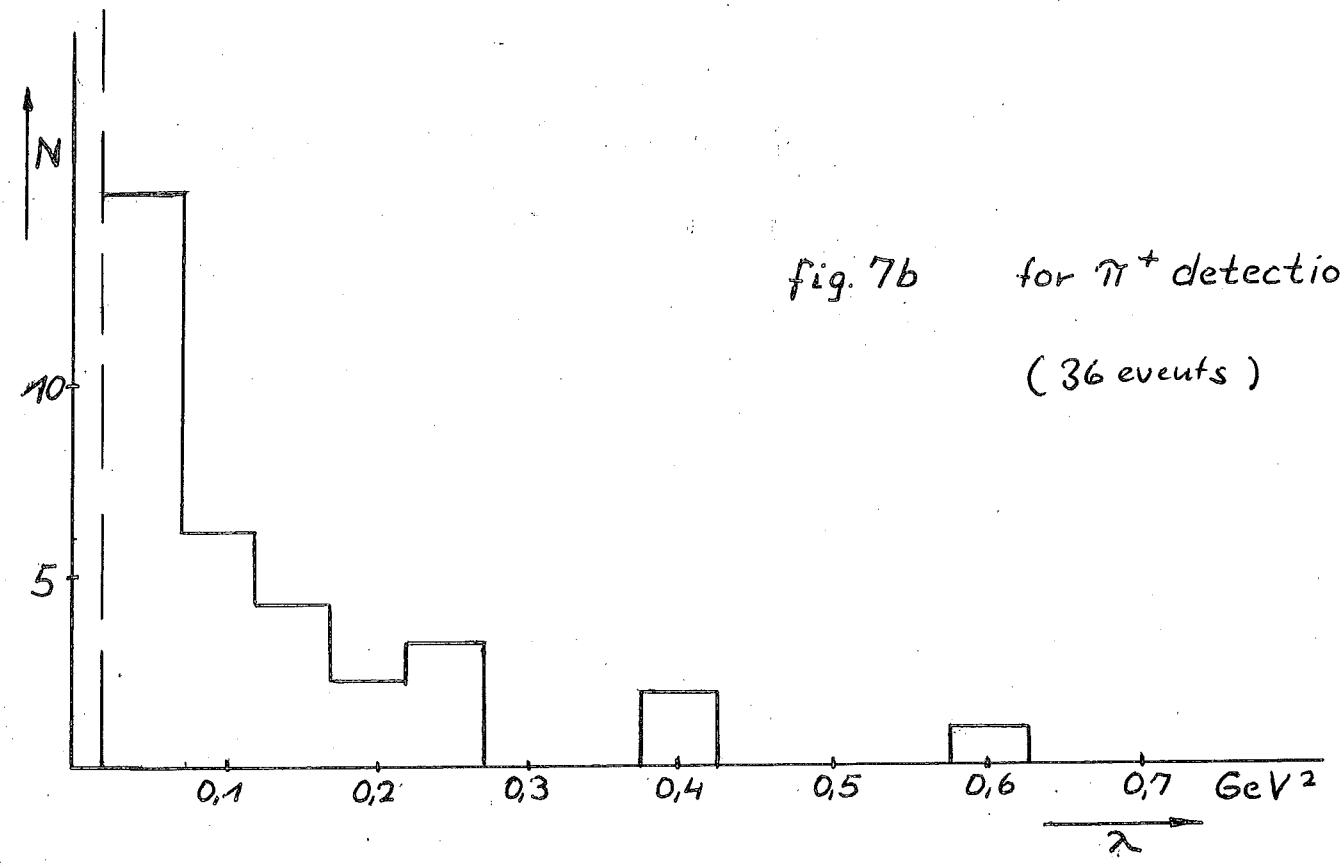

fig. 7b for π^+ detection

(36 events)

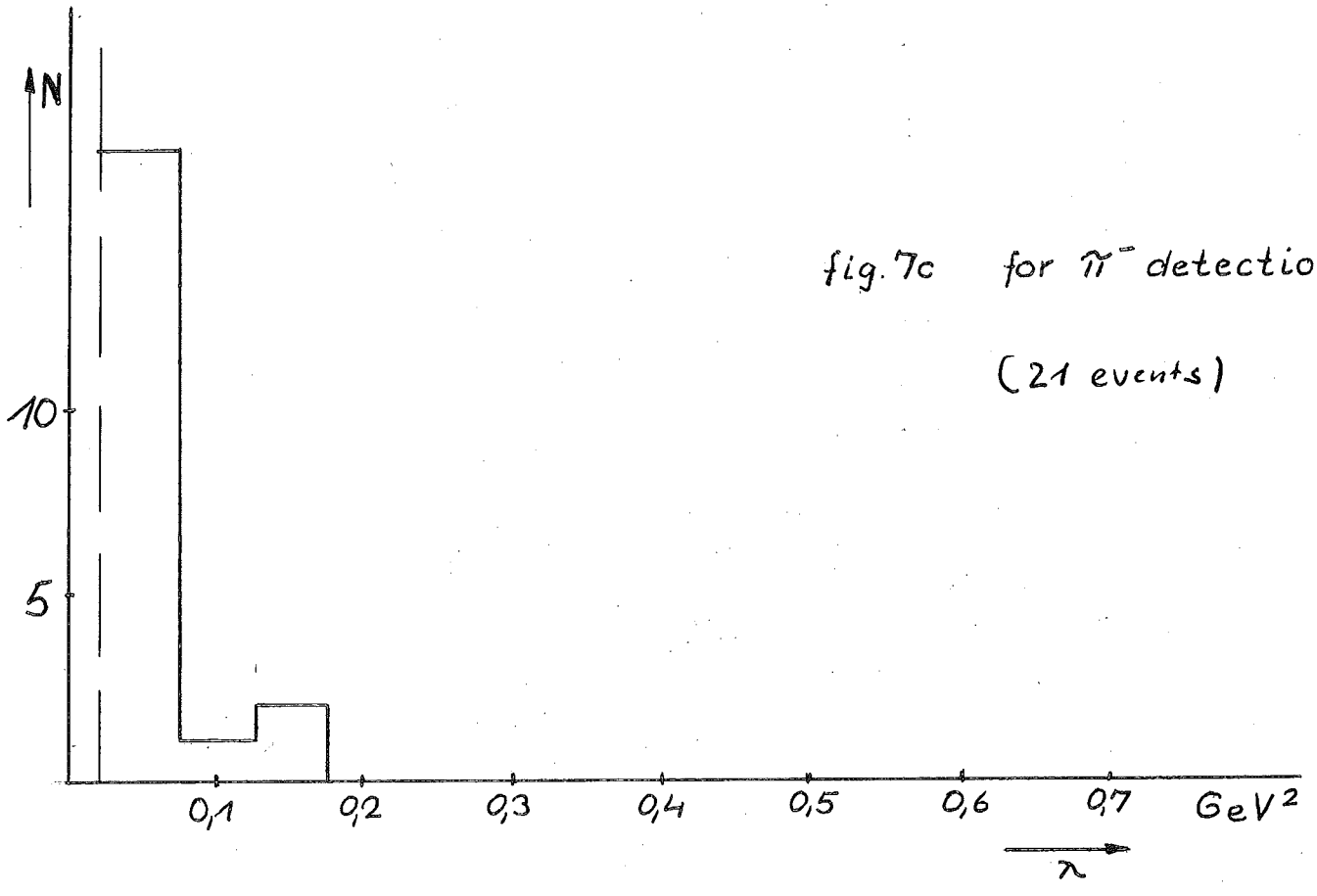

fig. 7c for π^- detection

(21 events)

Production Angle of the $\hat{\pi}$-Meson with Respect to the Direction of the Virtual Photon in Single $\hat{\pi}$-Production as a Function of the Momentum of the $\hat{\pi}$-Meson.
(Solid Curve Indicates the Mean Production Angle for One-$\hat{\pi}$-Exchange.)

fig. 8

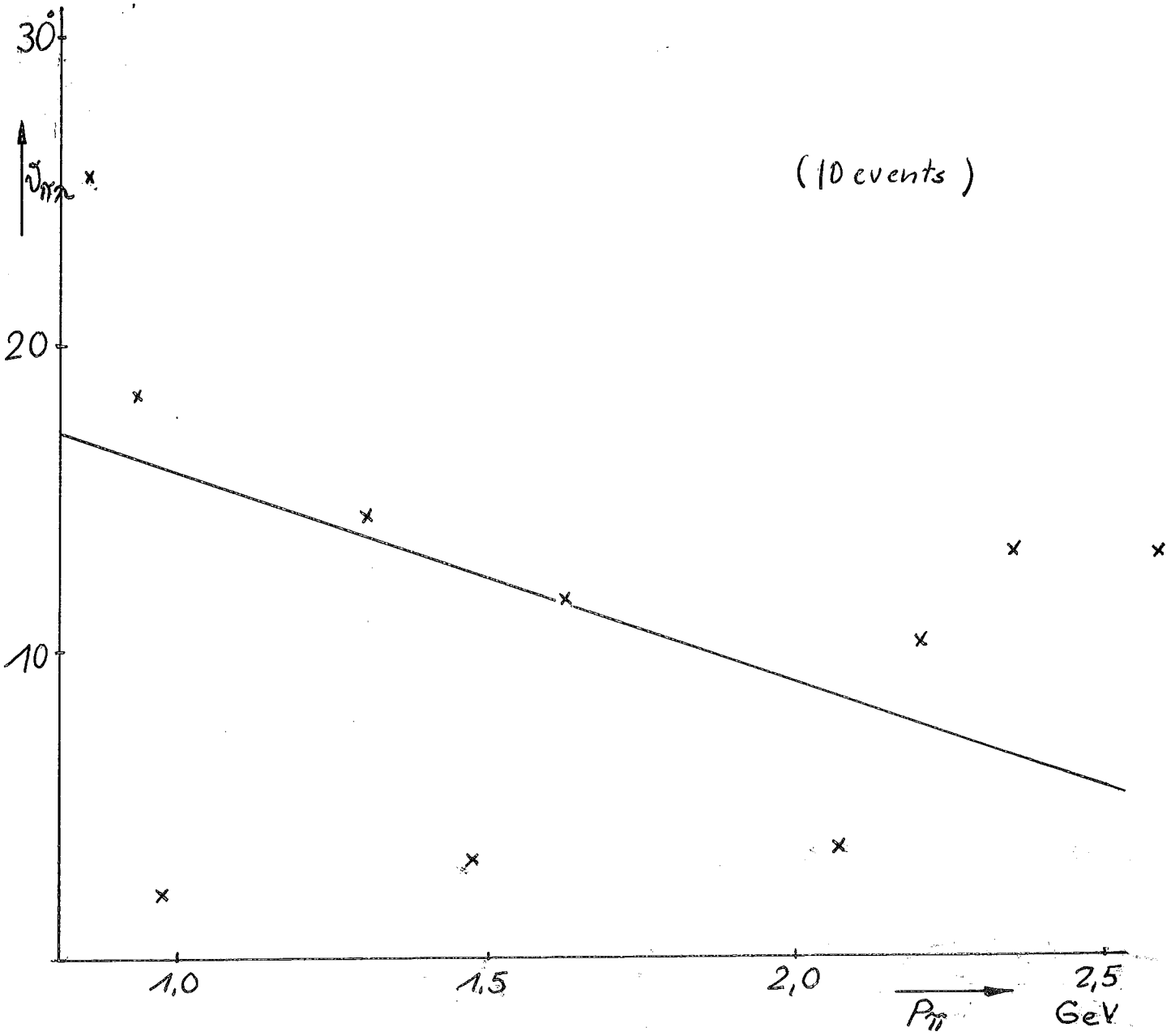

Resonant Nucleon Mass in Single π - Prod.

fig. 9

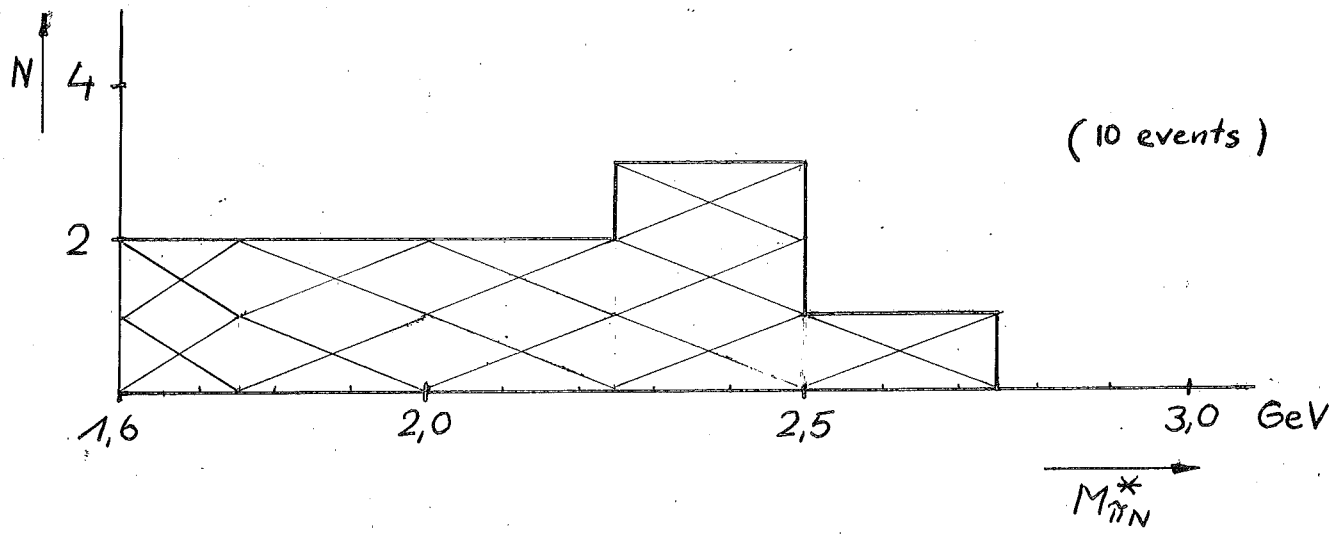

Resonant Nucleon Mass in Multiple π - Prod.

fig. 10

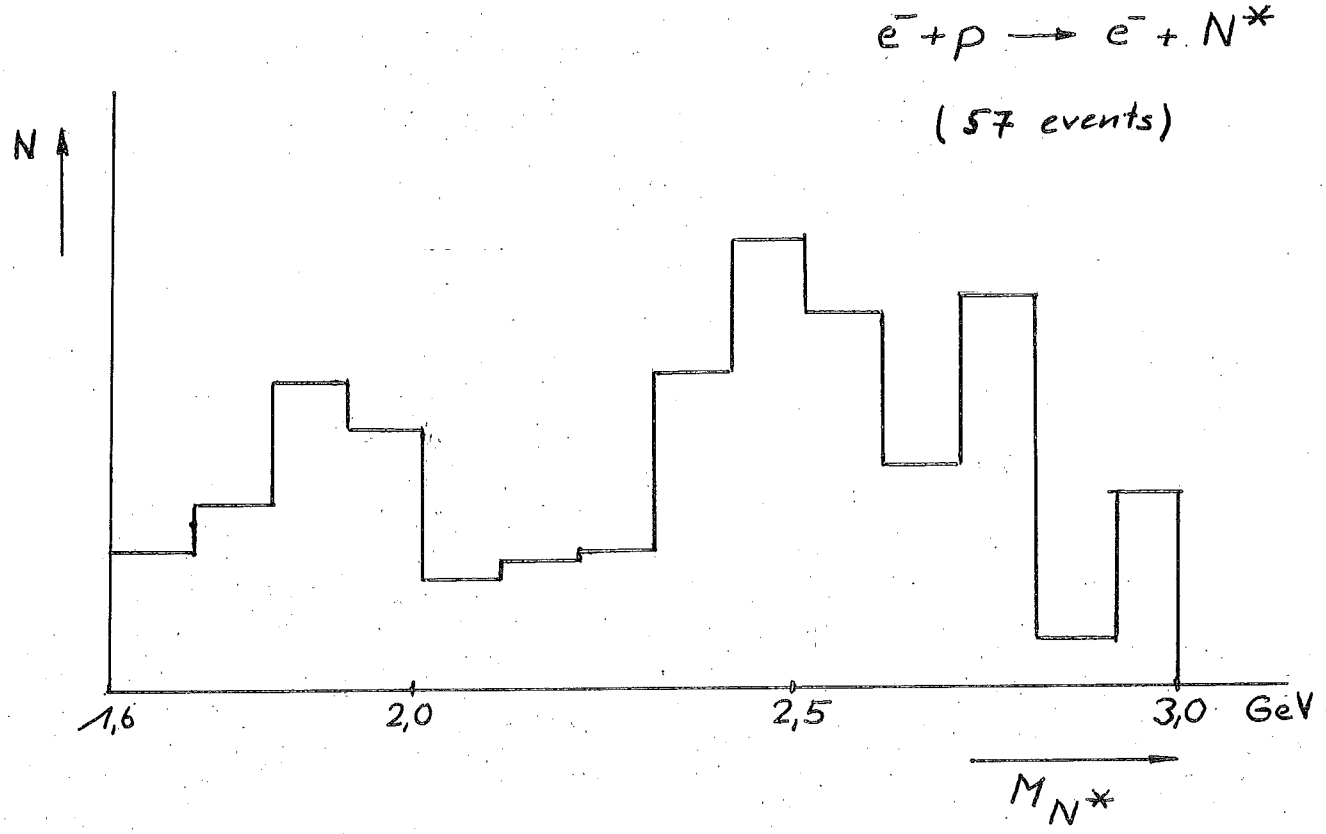

Resonant Mass M* / Missing Mass M' in Multiple π - Production

fig. 11

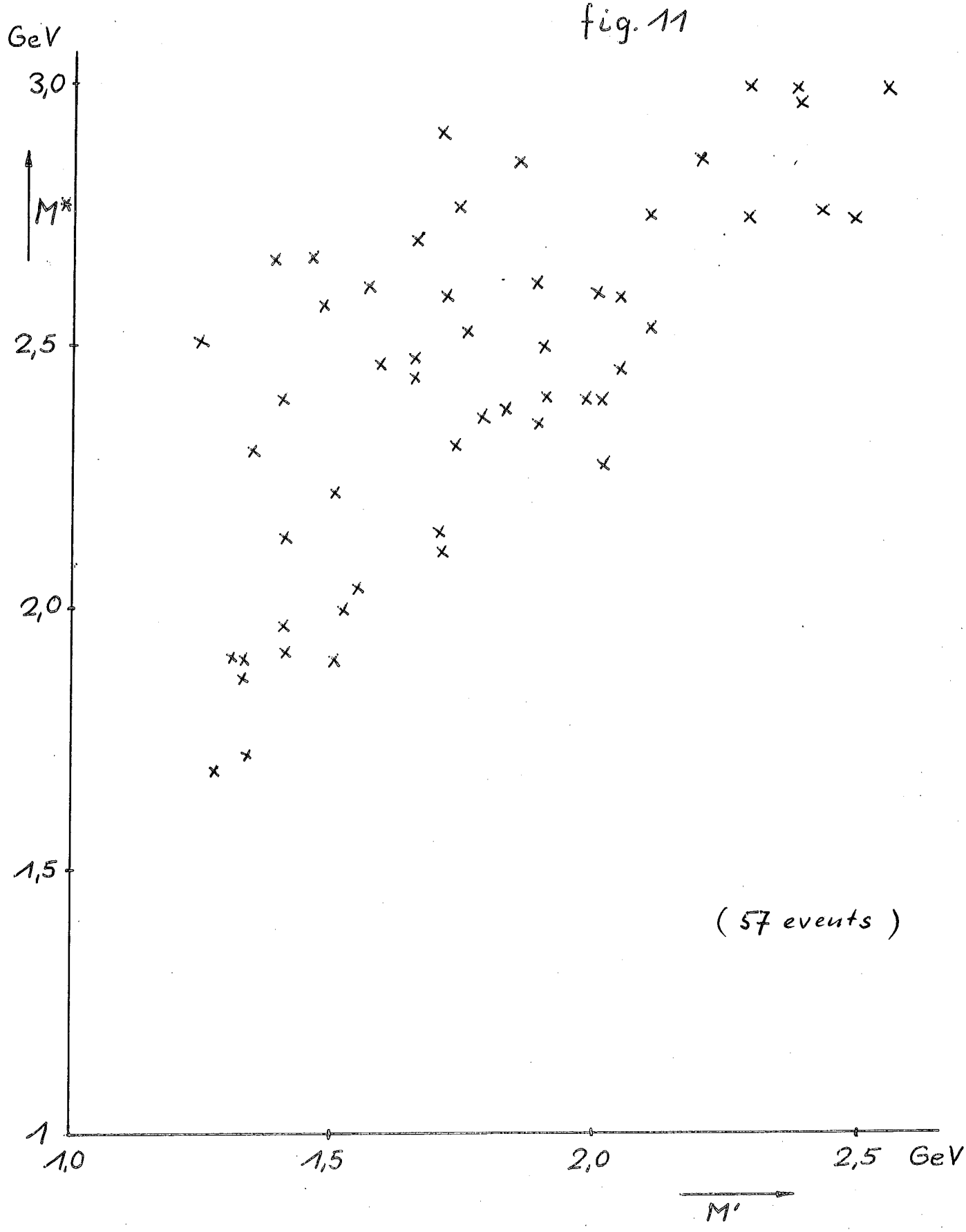

Mass-Spectrum of Dipions

fig. 12

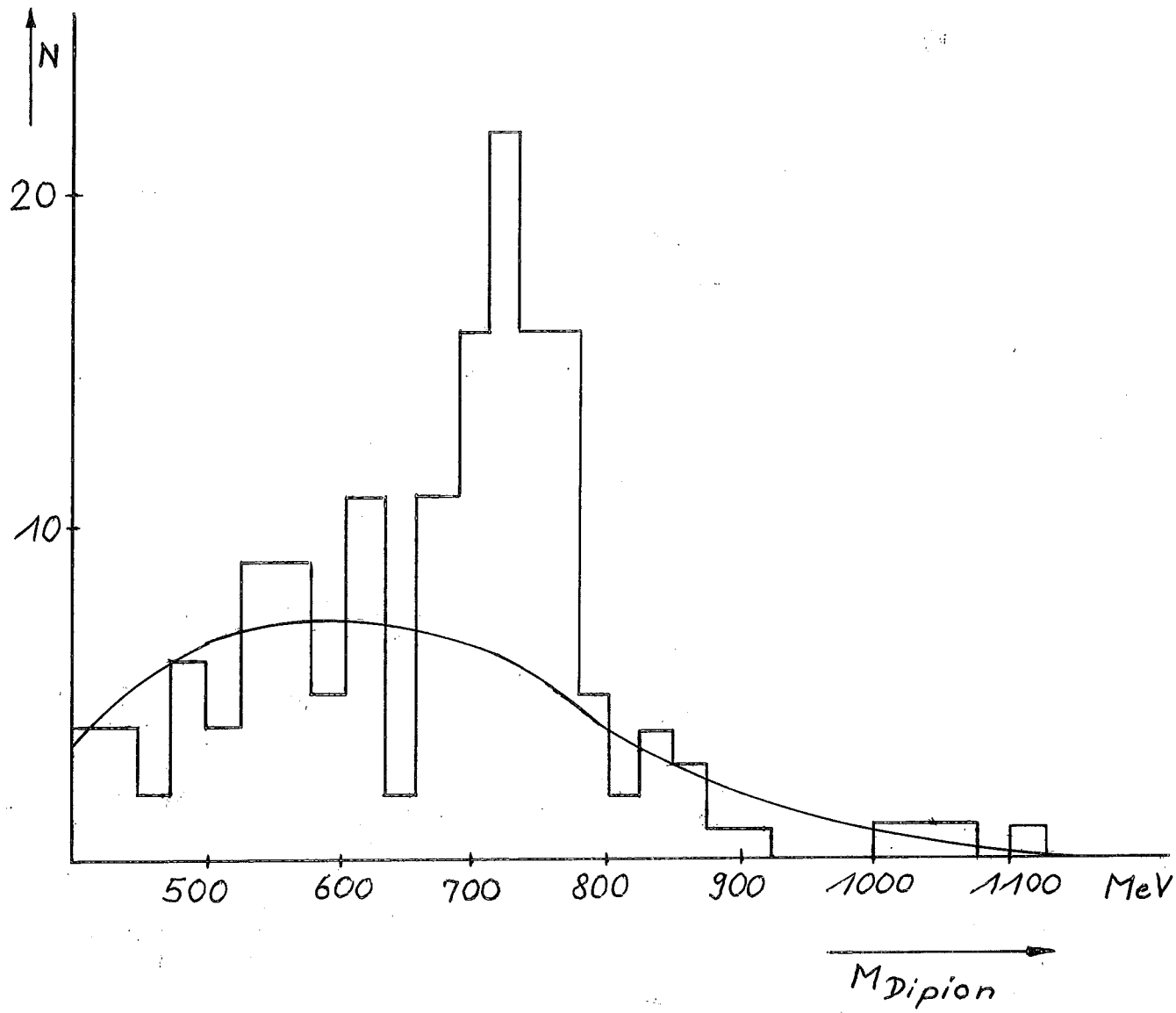

References:

(1) C.W.Akerlof, W.W.Ash, K.Berkelman, M.Tigner
Proc.of Sympos. on Electron and Photon Interactions at High Energies Hamburg 1965 (to be publ.)

(2) H.Lynch, J.V.Allaby, D.Ritson
Proc. of Symp. on Electron and Photon Interactions at High Energies Hamburg 1965

A.A.Cone, K.W.Chen, J.R.Dunning, G.Hartwig, N.F.Ramsey, J.K.Walker, Richard Wilson
PRL 14, 326 (1965)

L.N.Hand PR 129, 1834
G.G.Ohlsen PR 120, 584
W.K.H.Panofsky, E.Allton PR 110, 1155

(3) An earlier report on preliminary results of this experiment was given at the Symp. on Electron and Photon Interactions at High Energies Hamburg 1965

(4) E.Bleuler, D.O.Caldwell, B.Elsner, D.Harting, L.W.Jones, W.C.Middelkoop, B.Zacharov, R.de Perl, L.C. Teng
Nucl.Instr.a.Methods 20, 208, 1963

(5) D.O.Caldwell, J.P.Dowd, K.Heinloth, M.D.Rousseau
R.S.J. 36, 283 (1965)

(6) J.Müller thesis (1965) unpublished

(7) U.P.Reich thesis (1965) unpublished

(8) C. de Vries, R.Hofstadter, A.Johansson, R.Herman
PR 134, B 848 (1964)

(9) J.D.Jackson
Classical Electrodynamics
Section 15.6 (New York 1962)

(10) S.M.Berman
PR 135, B 1269 (1964)

(11) M.Gourdin
N.C. 37, 208 (1965) and Proc. of Symp.on Electron and Photon Interactions at High Energies Hamburg 1965

(12) R.B.Curtis
PR 104, 211 (1956)

(13) R.L.Walker
Proceed. of the Conference on Photon Interactions Cambridge/Mass. (1963)

(14) S.D.Drell
PRL 5, 278 (1960)

(15) CEA bubble chamber group
Proc. of Sympos. on Electron and Photon Interactions at High Energies Hamburg 1965

(16) DESY bubble chamber group
preprint DESY 65/5 (1965)